

Why Are Learned Indexes So Effective but Sometimes Ineffective?

Qiyu Liu
Southwest University
qyliu.cs@gmail.com

Siyuan Han
HKUST
shanaj@connect.ust.hk

Yanlin Qi
HIT Shenzhen
yanlinqi7@gmail.com

Jingshu Peng
ByteDance
jingshu.peng@bytedance.com

Jin Li
Harvard University
jinli@g.harvard.edu

Longlong Lin
Southwest University
longlonglin@swu.edu.cn

Lei Chen
HKUST & HKUST (GZ)
leichen@cse.ust.hk

ABSTRACT

Learned indexes have attracted significant research interest due to their ability to offer better space-time trade-offs compared to traditional B+-tree variants. Among various learned indexes, the PGM-Index based on error-bounded piecewise linear approximation is an elegant data structure that has demonstrated *provably* superior performance over conventional B+-tree indexes. In this paper, we explore two interesting research questions regarding the PGM-Index: ❶ *Why are PGM-Indexes theoretically effective?* and ❷ *Why do PGM-Indexes underperform in practice?* For question ❶, we first prove that, for a set of N sorted keys, the PGM-Index can, with high probability, achieve a lookup time of $O(\log \log N)$ while using $O(N)$ space. To the best of our knowledge, this is the **tightest bound** for learned indexes to date. For question ❷, we identify that querying PGM-Indexes is highly memory-bound, where the internal error-bounded search operations often become the bottleneck. To fill the performance gap, we propose PGM++, a *simple yet effective* extension to the original PGM-Index that employs a mixture of different search strategies, with hyper-parameters automatically tuned through a calibrated cost model. Extensive experiments on real workloads demonstrate that PGM++ establishes a new Pareto frontier. At comparable space costs, PGM++ speeds up index lookup queries by up to 2.31 \times and 1.56 \times when compared to the original PGM-Index and state-of-the-art learned indexes.

PVLDB Reference Format:

Qiyu Liu, Siyuan Han, Yanlin Qi, Jingshu Peng, Jin Li, Longlong Lin, and Lei Chen. Why Are Learned Indexes So Effective but Sometimes Ineffective?. PVLDB, 14(1): XXX-XXX, 2020.
doi:XX.XX/XXX.XX

PVLDB Artifact Availability:

The source code, data, and/or other artifacts have been made available at https://github.com/qyliu-hkust/bench_search.

1 INTRODUCTION

Indexes are fundamental components of DBMS and big data engines to enable real-time analytics [30, 35]. An emerging research tendency is to directly learn the storage layout of sorted data by using simple machine learning (ML) models, leading to the concept

This work is licensed under the Creative Commons BY-NC-ND 4.0 International License. Visit <https://creativecommons.org/licenses/by-nc-nd/4.0/> to view a copy of this license. For any use beyond those covered by this license, obtain permission by emailing info@vldb.org. Copyright is held by the owner/author(s). Publication rights licensed to the VLDB Endowment.

Proceedings of the VLDB Endowment, Vol. 14, No. 1 ISSN 2150-8097.
doi:XX.XX/XXX.XX

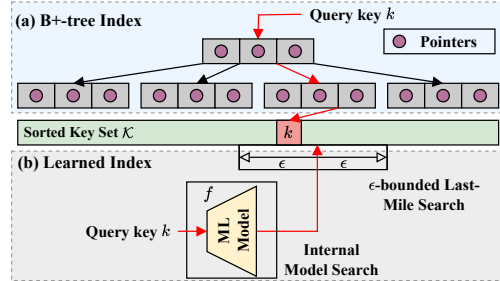


Figure 1: (a) A conventional B+-tree index. (b) A learned index with a “last-mile” maximum search error ϵ .

of *Learned Index* [8, 11, 18, 45, 50, 52]. Compared to traditional indexes like B+-tree variants [6, 14, 19], learned indexes have been shown to reduce the memory footprint by 2–3 orders of magnitude while achieving comparable index lookup performance.

Similar to B+-trees or other binary search tree (BST) variants, learned indexes address the classical problem of *Sorted Dictionary Indexing* [7]. Given an array of N sorted keys $\mathcal{K} = \{k_1, \dots, k_N\}$, the objective of learned indexes is to find a projection function (i.e., an ML model) $f(k) \in \mathbb{N}^+$ that maps an arbitrary query key k to its corresponding index in the sorted array \mathcal{K} (i.e., its position on storage). However, ML models inherently produce prediction errors. As illustrated in Figure 1, the maximum prediction error over \mathcal{K} is denoted by ϵ . To ensure the correctness of an index lookup query for a search key k , an exact “last-mile” search, typically a standard binary search, must be performed within the error range (i.e., $[f(k) - \epsilon, f(k) + \epsilon]$). To balance model accuracy with complexity, learned indexes such as Recursive Model Index (RMI) [18] and PGM-Index [11] opt to stack simple models, such as linear models or polynomial splines, in a hierarchical structure, thereby achieving a balance between the model complexity and fitting accuracy.

Among the various published learned indexes [8, 11, 18, 45, 50, 52], the PGM-Index [11] stands out as a simple yet elegant structure that has been proven to be *theoretically* more efficient than a B+-tree. As depicted in Figure 2, the PGM-Index is a multi-level structure constructed by recursively fitting *error-bounded piecewise linear approximation* models (ϵ -PLA). Searching in a PGM-Index is performed through a sequence of *error-bounded search* operations in a top-down manner. Recent theoretical analysis [10] indicates that, compared to a B+-tree with fanout B , the PGM-Index, however, can reduce memory footprint by a factor of B , while preserving the same logarithmic index lookup complexity (i.e., $O(\log N)$).

Intuitively, the PGM-Index is structured as a hierarchy of line segments, where the index height is a key factor in determining the lookup time complexity. Existing results [10, 11] suggest that the

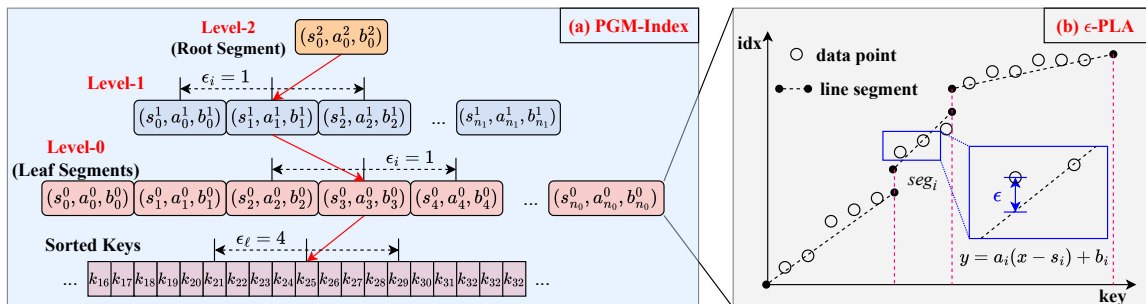


Figure 2: A toy example of a 3-level PGM-Index with $\epsilon_i = 1$ (i.e., internal search error range) and $\epsilon_\ell = 4$ (i.e., last-mile search error range). Processing a lookup query on such PGM-Index involves in total three linear function evaluations, two internal search operations in the range $2 \cdot \epsilon_i + 1$, and one “last-mile” search operation on the sorted data array in the range $2 \cdot \epsilon_\ell + 1$.

height of a PGM-Index built on N sorted keys should be $O(\log N)$. However, our empirical investigations reveal that PGM-Indexes are highly *flat*, with over **99%** of the total index space cost attributed to the segments at the *bottom* level. This observation implies that the height of the PGM-Index grows more slowly than $O(\log N)$, potentially at a sub-logarithmic rate. Motivated by this, we pose the following research question.

Q1: Why Are PGM-Indexes So Effective in Theory? To answer this question, we establish new theoretical results for PGM-Indexes. With high probability (w.h.p.), the index lookup time can be bounded by $O(\log_2 \log_G N) = O(\log \log N)$ using linear space of $O(N/G)$, where G is a constant determined by data distribution characteristics and the error constraint ϵ . To the best of our knowledge, this work presents the *tightest* bound for learned index structures compared to existing theoretical analyses [10, 49].

Interestingly, BSTs can be viewed as a “materialized” version of the binary search algorithm, whose time complexity is $O(\log N)$. As an analog, the PGM-Index with piecewise linear approximation models can be regarded as a “materialized” version of the interpolation search algorithm, whose time complexity is $O(\log \log N)$ [27, 33], aligning with our theoretical findings.

Despite its theoretical superiority, recent benchmarks [22, 44] show that the PGM-Index falls short of practical performance expectations, often underperforming compared to well-optimized RMI variants [17, 18]. This leads to our second research question.

Q2: Why Are PGM-Indexes Ineffective in Practice? Our investigation into extensive benchmark results across various hardware platforms reveals that PGM-Indexes are memory-bound. The internal error-bounded search operation, often implemented as a standard binary search (e.g., `std::lower_bound` in C++), becomes a bottleneck when processing an index lookup query. According to our benchmark (Section 5), less than **1%** of the internal segments account for over **80%** of the total index lookup time.

To improve search efficiency, we propose a hybrid internal search strategy that combines the advantages of linear search and highly optimized branchless binary search by properly setting search range thresholds. Additionally, as illustrated in Figure 2, constructing a PGM-Index necessitates two hyper-parameters ϵ_i and ϵ_ℓ , the error thresholds for internal index traversal and last-mile search on the data array, respectively. We find that the ϵ_ℓ primarily controls the overall index size, while both ϵ_i and ϵ_ℓ influence the index lookup efficiency. Based on theoretical analysis and experimental observations, we develop a cost model that is finely calibrated using

benchmark data. Leveraging this cost model, we further introduce an automatic hyper-parameter tuning strategy to better balance index lookup efficiency with index size.

In summary, our technical contributions are as follows. **1 New Bound.** We prove the sub-logarithmic index lookup time of the PGM-Index (i.e., $O(\log \log N)$). This result tightens the previous logarithmic bound on the PGM-Index and further validates its provable performance superiority compared to conventional tree-based indexes. **2 Simple Methods.** We introduce PGM++, a *simple yet effective* improvement to the PGM-Index by replacing the costly internal search operations. We further devise an automatic parameter tuner for PGM++, guided by an accurate cost model. **3 New Pareto Frontier.** Extensive experimental studies on real and synthetic data show that, with a comparable index memory footprint, PGM++ robustly outperforms the original PGM-Index and optimized RMI variants [22, 50] by up to **2.31×** and **1.56×**, respectively. For example, even on a resource-constrained device like MacBook Air 2024 [21], PGM++ achieves index lookup time of **<400 ns** on **800 million** keys, using only **0.28 MB** of memory.

The remainder of this paper is structured as follows. Section 2 introduces the basis of learned indexes, followed by the micro-benchmark setup details in Section 3. Section 4 presents our core theoretical analysis of the PGM-Index. Section 5 explores the reasons behind the PGM-Index’s underperformance in practice. In Section 6, we introduce PGM++, an optimized PGM-Index variant featuring hybrid error-bounded search and automatic hyper-parameter tuning. Section 7 reports the experimental results. Section 8 surveys and discusses related works, and finally, Section 9 concludes the paper and discusses future studies.

2 PRELIMINARIES

We first overview the basis of learned indexes (\triangleright Section 2.1) and then elaborate on the details of existing theoretical results (\triangleright Section 2.2). Table 1 summarizes the major notations.

2.1 Learned Index

Given a set of N sorted keys $\mathcal{K} = \{k_1, k_2, \dots, k_N\}$ and an index set $\mathcal{I} = \{1, 2, \dots, N\}$, the goal of learned indexes is to find a mapping function $f(k) \in \mathbb{N}^+$ such that f can project a search key $k \in \mathcal{K}$ to its corresponding index rank $\text{rank}(k) \in \mathcal{I}$ with controllable error. Intuitively, learning f is equivalent to learning a cumulative distribution function (CDF) scaled by the data size N . The model selection considerations for f are threefold:

Table 1: Summary of major notations.

Notation	Description
\mathcal{K}	a set of N sorted keys
$\text{rank}(k)$	the sorting index of a key k in \mathcal{K}
ϵ_i	the internal search error parameter of PGM-Index
ϵ_ℓ	the last-mile search error parameter of PGM-Index
g_i	the difference between k_i and k_{i-1} (a.k.a. gap)
μ, σ^2	the mean and variance of gap distribution
(s, a, b)	a line segment $\ell(x) = a \cdot (x - s) + b$
H_{PGM}	the height of a PGM-Index

❶ **Compactness:** the model f should be compact to reduce memory footprint, and model inference using f must not introduce significant computational overhead;

❷ **Error-Boundedness:** the model f should be error-bounded, ensuring that an exact last-mile search can correct prediction errors, i.e., $|f(k) - \text{rank}(k)| \leq \epsilon$ for $\forall k \in \mathcal{K}$;

❸ **Monotonicity:** to ensure the correctness of querying keys outside \mathcal{K} , $f(k_1) \leq f(k_2)$ should hold for any $k_1 \leq k_2$.

Since running deep learning (DL) models usually require a heavy runtime like PyTorch [31] or TensorFlow [37] that are costly and less flexible, existing learned index designs favor *stacking* simple models, such as linear functions [8, 11, 45], polynomial splines [18], and radix splines [17]. Among these learned index structures, the PGM-Index [11] employs the error-bounded piecewise linear approximation (ϵ -PLA) to strike a balance between the model complexity and prediction accuracy, which is defined as follows.

Definition 2.1 (ϵ -PLA). Given a univariate set $\mathcal{X} = \{x_1, \dots, x_N\}$, a corresponding target set $\mathcal{Y} = \{y_1, \dots, y_N\}$, and an error constraint ϵ , an ϵ -PLA on the point set in Cartesian space $(\mathcal{X}, \mathcal{Y}) = \{(x_i, y_i)\}_{i=1, \dots, N}$ is defined as,

$$f(x) = \begin{cases} a_1 \cdot (x - s_1) + b_1 & \text{if } s_1 \leq x < s_2 \\ a_2 \cdot (x - s_2) + b_2 & \text{if } s_2 \leq x < s_3 \\ \dots & \dots \\ a_m \cdot (x - s_m) + b_m & \text{if } s_m \leq x < +\infty \end{cases} \quad (1)$$

such that for $\forall i = 1, 2, \dots, N$, it always holds that $|f(x_i) - y_i| \leq \epsilon$.

The i -th segment in Eq. (1) can be expressed by a tuple $\text{seg}_i = (s_i, a_i, b_i)$ where s_i is the segment starting point, a_i is the slope, and b_i is the intercept. To ensure the monotonic requirement, the segments in Eq. (1) should satisfy two conditions: (a) $a_i \geq 0$ for $i = 1, \dots, m$, and (b) $s_i < s_j$ for $\forall 1 \leq i < j \leq m$. We then extend the original PGM-Index definition [11] by separating the error parameters for internal search and last-mile search.

Definition 2.2 ($(\epsilon_i, \epsilon_\ell)$ -PGM-Index [11]). Given a sorted key set $\mathcal{K} = \{k_1, k_2, \dots, k_N\}$ and two error parameters ϵ_i and ϵ_ℓ ($\epsilon_i, \epsilon_\ell \in \mathbb{N}^+$), an $(\epsilon_i, \epsilon_\ell)$ -PGM-Index is a multi-level structure where the bottom level (a.k.a., the leaf level or level-0) is an ϵ_ℓ -PLA and the remaining levels (a.k.a., internal levels) are ϵ_i -PLA(s). The structure can be constructed in a *bottom-up* manner:

- ❶ **Leaf Level:** an ϵ_ℓ -PLA constructed on $(\mathcal{K}, \mathcal{I} = \{1, \dots, N\})$.
- ❷ **Internal Levels:** for the j -th level ($j \geq 1$), let \mathcal{S}_{j-1} denote the set of segments in the $(j-1)$ -th level (i.e., the previous level), and let $\mathcal{K}_{j-1} = \{\text{seg.s} \mid \text{seg} \in \mathcal{S}_{j-1}\}$ and $\mathcal{I}_{j-1} = \{1, 2, \dots, |\mathcal{K}_{j-1}|\}$. Then, the j -th level is an ϵ_i -PLA constructed on dataset $(\mathcal{K}_{j-1}, \mathcal{I}_{j-1})$.
- ❸ **Root Level:** the internal level consisting of a *single* line segment.

Table 2: Summary of theoretical results. For our result, G is a constant that depends on data distribution characteristics and the pre-specified error bound ϵ .

Results	Base Model	Lookup Time	Space Cost
ICML'20 [10]	Linear	$O(\log N)$	$O(N/\epsilon^2)$
ICML'23 [49]	Constant	$O(\log \log N)$	$O(N \log N)$
Ours	Linear	$O(\log \log N)$	$O(N/G)$

Specifically, we denote the segments in the bottom level as *leaf segments* and the remaining segments as *internal segments* (corresponding to the subscripts of ϵ_ℓ and ϵ_i , respectively). The following example illustrates the PGM-Index lookup query processing.

Example 2.3 (PGM-Index Lookup). Figure 2 illustrates a 3-level PGM-Index with $\epsilon_i = 1$ and $\epsilon_\ell = 4$. Given a query key k , an index lookup query is performed in a *top-down* manner from the root level to the bottom level as follows:

❶ **The Internal Index Traversal** phase starts from the root level and finds the appropriate line segment in each level until reaching the bottom level (depicted by the red path in Figure 2). Specifically, let $\text{seg}^j = (s^j, a^j, b^j)$ denote the segment in the j -th level during the traversal. The next segment in the $(j-1)$ -th level to be traversed is found by searching k within range $a^j \cdot (k - s^j) + b^j \pm \epsilon_i$.

❷ **The Last-Mile Search** phase performs an exact search on the raw sorted keys (i.e., \mathcal{K}) within the range $\overline{\text{rank}(k)} \pm \epsilon_\ell$ where $\overline{\text{rank}(k)} = a^0 \cdot (k - s^0) + b^0$ is the predicted rank and $\text{seg}^0 = (s^0, a^0, b^0)$ is the *leaf segment* found during the internal index traversal phase.

Recall that the index construction procedures introduced in Definition 2.2 guarantees that the maximum errors for internal index traversal and last-mile search cannot exceed ϵ_i and ϵ_ℓ , respectively. Thus, the aforementioned lookup processing ensures the correct location (i.e., $\text{rank}(k)$) must be found for an arbitrary query key k .

2.2 Existing Theoretical Results

From Section 2.1, two key questions need to be addressed to determine the space and time complexities of the PGM-Index. ❶ *How many line segments are required to satisfy the error constraint for an ϵ -PLA model?* and ❷ *What is the height (i.e., the number of layers) of a PGM-Index?* In this section, we review the related theoretical studies [10, 49] regarding these two questions, with major results summarized in Table 2.

The original PGM-Index [11] first provides a straightforward lower bound to determine the index height.

THEOREM 2.4 (PGM-INDEX LOWER BOUND [11]). *Given a consecutive chunk of $2\epsilon + 1$ sorted keys $\{k_i, \dots, k_{i+2\epsilon}\} \subseteq \mathcal{K}$, there exists a horizontal line segment $\ell(x) = i + \epsilon$ such that $|\ell(k_j) - j| \leq \epsilon$ holds for $j = i, \dots, i + 2\epsilon$, implying that each line segment in an ϵ -PLA can cover at least $2\epsilon + 1$ keys.*

Recall the recursive construction process in Definition 2.2, w.l.o.g., a PGM-Index with $\epsilon_i = \epsilon_\ell = \epsilon$ has a height of $O(\log_\epsilon N) = O(\log N)$. Thus, the index lookup takes time $O(\log N \cdot \log_2 \epsilon) = O(\log N)$ as ϵ can be regarded as a pre-specified constant.

Ferragina et al. [10] further tighten the results in Theorem 2.4 by showing that the expected segment coverage is proportional to ϵ^2 . Suppose that the key set to be indexed $\mathcal{K} = \{k_1, k_2, \dots, k_N\}$ is a materialization of a random process $k_i = k_{i-1} + g_i$ for $i \geq 2$

Table 3: Summary of three micro-benchmark platforms. For platforms X86-1 and ARM whose CPU chips adopt the “big.LITTLE” architecture [3], the hardware statistics of the performance cores (i.e., P-core) are reported. The reported L1/L2/L3 sizes represent the actual cache size that a physical core can access. Notably, for the Apple M3 chip, only L1 cache and L2 cache are available.

Platform	OS	Compiler	CPU	Frequency	Memory	L1	L2	L3 (LLC)
X86-1	Ubuntu 20.04	g++ 11	Intel Core i7-13700K	5.30 GHz (P-core)	32 GB DDR4	64 KiB	256 KiB	16 MB
X86-2	CentOS 9.4	g++ 11	AMD EPYC 7413	3.60 GHz	1 TB DDR4	64 KiB	1 MB	256 MB
ARM	macOS 14.4.1	clang++ 15	Apple M3	4.05 GHz (P-core)	16 GB LPDDR5	320 KiB	16 MB	N.A.

where g_i 's are i.i.d. random variables (r.v.) following some unknown distribution. We term the r.v. g_i as the “gap” and denote $\mu = \mathbb{E}[g_i]$ and $\sigma^2 = \text{Var}[g_i]$ as its mean and variance. These distribution characteristics are crucial in determining the expected number of segments to satisfy the error constraints.

THEOREM 2.5 (EXPECTED LINE SEGMENT COVERAGE [10]). *Given a set of sorted keys $\mathcal{K} = \{k_1, k_2, \dots, k_N\}$ and an error parameter ϵ , let the gap be $g_i = k_i - k_{i-1}$. If the condition $\epsilon \gg \sigma/\mu$ holds, with high probability, the expected number of keys in \mathcal{K} covered by a line segment $\ell(x) = \mu \cdot (x - k_1) + 1$ is given by*

$$\mathbb{E} \left[\min \{i \in \mathbb{N}^+ \mid |\ell(k_i) - i| > \epsilon\} \right] = \mu^2 \epsilon^2 / \sigma^2, \quad (2)$$

where $\ell(k_i) = \mu \cdot (k_i - k_1) + 1$ is the predicted index for a key k_i .

By constructing a special line segment with slope μ , Theorem 2.5 establishes the relationship between the expected segment coverage and the error constraint ϵ . Based on Theorem 2.5, for a set of N sorted keys, the expected number of segments¹ of a *one-layer* ϵ -PLA can be derived as $N\sigma^2/\epsilon^2\mu^2$. In the practical PGM-Index implementation, an *optimal* ϵ -PLA fitting algorithm [26] is adopted to *minimize* the number of line segments while ensuring the error constraint ϵ is met. Thus, the expected number of segments can be then bounded by $O(N\sigma^2/\epsilon^2\mu^2)$.

Combining the results in Theorem 2.4 and Theorem 2.5, Ferragina et al. [10] conclude that a PGM-Index with $\epsilon_i = \epsilon_\ell = \epsilon$ using $O(N/\epsilon^2)$ space can handle lookup queries in $O(\log N)$ time with high probability. By setting $\epsilon = \Theta(B)$, a PGM-Index can achieve the same logarithmic index lookup complexity of a B+-tree while reducing the space complexity from B+-tree’s $O(N/B)$ to $O(N/B^2)$.

In addition to [10], a recent study [49] also delves into the theoretical aspects of learned index. They demonstrate that a Recursive Model Index [18] using *piece-wise constant* functions as base models can achieve a sub-logarithmic lookup complexity of $O(\log \log N)$ at the cost of *super-linear* space, specifically $O(N \log N)$.

Our Results. Inspired by the findings in [49], we reasonably speculate that PGM-Indexes, utilizing ϵ -PLA as base models, can achieve the same *sub-logarithmic* lookup time complexity with *reduced* space overhead, given that a constant function can be regarded as a special case of a piecewise linear function. As summarized in Table 2, our analysis in Section 4 concludes that, w.h.p., the PGM-Index can search a query key in $O(\log \log N)$ time while requiring only linear space $O(N/G)$, where G is a constant related to the error parameter ϵ and gap distribution characteristics.

3 MICROBENCHMARK SETTING

To ensure consistency in presentation, this section outlines the microbenchmark setups, including the hardware platforms, datasets,

¹The conclusion is drawn hastily as, in general, $1/\mathbb{E}[X] \neq \mathbb{E}[1/X]$ for an arbitrary random variable X . A more rigorous proof can be found in Theorem 4 of [10].

Table 4: Statistics of benchmark datasets. h_D is the distribution hardness ratio. \overline{Cov} is the observed segment coverage to fit a PLA model with an error bound of $\epsilon = 16$.

Dataset	Category	#Keys	Raw Size	h_D	\overline{Cov}
fb	Real	200 M	1.6 GB	3.88	94
wiki	Real	200 M	1.6 GB	1.77	877
books	Real	800 M	6.4 GB	5.39	101
osm	Real	800 M	6.4 GB	1.91	129

and query workloads. The remainder of this paper adopts this microbenchmark to either motivate or validate the theoretical findings and proposed methodologies.

Platforms. We perform the subsequent experiments on three platforms with different architectures: ❶ X86-1 is an Ubuntu desktop equipped with an Intel® Core™ i7-13700K CPU (5.30 GHz, P-core) and 64 GB of memory; ❷ X86-2 is a CentOS server with 2 AMD® EPYC™ 7413 CPUs (3.60 GHz) and 1 TB of memory; and ❸ ARM is a Macbook Air laptop with an Apple Silicon M3 CPU (4.05 GHz, P-core) and 16 GB of unified memory, which offers higher memory bandwidth compared to the X86 platforms. As we will discuss in Section 5, searching a PGM-Index is highly memory-bound, and factors such as cache latency and memory bandwidth can significantly affect query performance². Table 3 summarizes the specifications of the benchmark platforms.

In addition, all the experiments are written in C++ and compiled using g++ 11.4 on X86-1 and X86-2 and clang++ 15 on ARM. The complete microbenchmark implementation and experimental results are publicly available at [28].

Benchmark Datasets. We adopt 4 real datasets from SOSD [22] that have been widely evaluated in previous studies [8, 17, 44, 45, 50]. Specifically, ❶ fb is a set of user IDs randomly sampled from Facebook [33]; ❷ wiki is a set of edit timestamp IDs committed to Wikipedia [42]; ❸ books is the dataset of book popularity from Amazon; and ❹ osm is a set of cell IDs from OpenStreetMap [25]. We also generate 3 synthetic datasets by sampling from uniform, normal, and log-normal distributions, following a process similar to [22, 52]. All keys are stored as 64-bit unsigned integers (`uint64_t` in C++), and Table 4 summarizes the dataset statistics.

To quantify the difficulty of indexing a dataset, we define the *distribution hardness ratio* as $h_D = \sigma^2/\mu^2$ where μ and σ^2 represent the mean and variance of the gap distribution for a dataset. According to Theorem 2.5, a higher h_D implies a harder dataset to learn, as more segments are required to meet the error constraint ϵ . However, as illustrated in Figure 3, extreme values can easily influence h_D , leading to an overestimation of the necessary segment count. For example, on dataset osm, the original hardness ratio $h_D = 1.27 \times 10^6$, and according to Theorem 2.5, the expected segment coverage for

²Typical access latencies for L1 cache, last level cache (LLC), and main memory are 1 ns, 20 ns, and 100 ns, respectively.

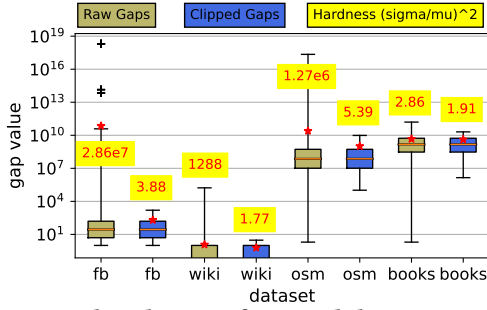


Figure 3: Gap distributions for 4 real datasets. In the box plots, the horizontal lines and the star marks refer to the medians and means of data, respectively.

an ϵ -PLA with $\epsilon = 16$ can be estimated as,

$$\frac{\mu^2 \cdot \epsilon^2}{\sigma^2} = \frac{\epsilon^2}{h_D} = \frac{16^2}{1.27 \times 10^6} \approx 0.0002, \quad (3)$$

which is far away from 129, the observed segment coverage.

To mitigate this, we clip the observed gaps at the 1%- and 99%-quantiles and re-calculate h_D based on the clipped gaps (as reported in column h_D of Table 4). After removing the extreme gaps, the revised $h_D = 5.39$ on dataset *osm*, and the corresponding estimated segment coverage is $16^2/5.39 \approx 71.3$, which is much closer to the observed value. Notably, accurately estimating the segment coverage is vital to building an effective cost model. The estimator based on clipped gaps remains too *coarse*, as it fails to capture local data variations. In Section 6.2, we will develop a more fine-grained coverage estimator based on adaptive data partition.

Query Workloads. Similar to the settings in [11, 17, 18, 50], our work focuses on *in-memory read-heavy* workloads. Given a key set \mathcal{K} , we generate the query workload by randomly sampling S (by default $S = 5,000$) keys from \mathcal{K} . To simulate different access patterns, we sample lookup keys from two distributions: ① *Uniform*, where every key in \mathcal{K} has an equal likelihood of being sampled; and ② *Zipfan*, where the probability of sampling the i -th key in \mathcal{K} is given by $p(i) = i^\alpha / \sum_{j=1}^N j^\alpha$. For the Zipfan workload, by default, we set the parameter $\alpha = 1.3$ such that over 90% of index accesses occur within the range of $(0, 10^3]$.

4 WHY ARE PGM-INDEXES SO EFFECTIVE?

In this section, we first motivate the necessity of an index height lower than $O(\log N)$ through benchmark results (\triangleright Section 4.1). Then, we establish a tighter sub-logarithmic bound (\triangleright Section 4.2). Finally, a case study on uniformly distributed keys is provided to further validate our theoretical analysis (\triangleright Section 4.3).

4.1 Motivation Experiments

We construct the PGM-Indexes and B+-trees using various configurations, with index statistics summarized in Table 5. Intuitively, a B+-tree with a fan-out of $B = \epsilon$ can be considered analogous to a PGM-Index where $\epsilon_i = \epsilon_\ell = \epsilon$, since a B+-tree index guarantees the search key to be located within a data block of size B .

As shown in Table 5, we first fix $B = \epsilon = 16$ while varying the input data size across $\{10^3, 10^4, \dots, 10^9\}$ using synthetic uniform keys. As the data size N increases, the height of a B+-tree index (H_B) follows a logarithmic growth pattern, adhering to the formula $H_B = \lceil 1 + \log_B \frac{N+1}{2} \rceil$. On the other hand, the PGM-Index height

Table 5: Statistics of PGM-Index ($\epsilon_i = \epsilon_\ell = \epsilon$) and B+-tree (fan-out $B = \epsilon$) under different configurations. ϵ is fixed to 8 when varying data size N (synthetic uniform keys), and N is fixed to 800M when varying ϵ (real dataset books). The ratio in percentage refers to the proportion of leaf segments contributing to the total index memory footprint.

N	PGM Height	Leaf Segments	Internal Segments	% over Total	B+-tree Height
10^3	2	2	2	50.0%	4
10^4	2	16	2	88.9%	6
10^5	2	140	2	98.6%	7
10^6	2	1,388	2	99.9%	8
10^7	3	13,918	12	99.9%	9
10^8	3	139,376	109	99.9%	10
10^9	4	1,394,003	1,049	99.9%	11

$\epsilon (B)$	PGM Height	Leaf Segments	Internal Segments	% over Total	B+-tree Height
8	4	16,859,902	46,572	99.7%	11
16	4	7,943,403	4,100	99.9%	9
32	3	2,464,229	272	99.99%	7
64	3	797,152	60	99.99%	6
128	3	267,966	25	99.99%	6
256	3	81,340	12	99.99%	5
512	3	22,684	7	99.99%	5

(H_{PGM}) grows at a much slower, sub-logarithmic rate. Besides, on dataset *books*, when varying ϵ within $\{2^2, 2^3, \dots, 2^{10}\}$, the results consistently demonstrate that $H_{PGM} \ll H_B$ holds across all ϵ configurations. Moreover, the decrease in H_{PGM} relative to ϵ is also notably slower than that of H_B . In addition to the index height, we also report the numbers of leaf and internal segments in Table 5. Unlike B+-trees or other BST variants, the PGM-Index exhibits a highly “flat” structure, with most of the line segments (up to 99.99%) located at the bottom level, aligning with its slow height growth.

Notably, the results obtained from different datasets and additional ϵ configurations are similar and therefore omitted here due to page limitations. The complete results are available at [28].

4.2 Theoretical Analysis

In this section, we aim to provide a new bound tightening the previous results. The road map for establishing our theoretical results is outlined below.

- ① Lemma 4.1 and Lemma 4.2 provide a lower bound for the expected segment coverage in an arbitrary level of the PGM-Index;
- ② Theorem 4.3 derives the PGM-Index height as $O(\log \log N)$, indicating sub-logarithmic growth w.r.t. the data size N ;
- ③ Theorem 4.4 concludes the space and time complexities of the PGM-Index as summarized in Table 2.

Notably, unless explicitly stated otherwise, the subsequent analyses adhere to the core assumptions regarding *gaps* from Theorem 2.5 [10], that is, the gaps are i.i.d. random variables following some unknown distribution with expectation μ and variance σ^2 . Besides, as discussed in [10], the “i.i.d.” assumption can be further relaxed to *weakly correlated* random variables without affecting the correctness of theoretical results.

LEMMA 4.1 (EXPECTED COVERAGE RECURSION). *Given a set of N sorted keys $\mathcal{K} = \{k_1, \dots, k_N\}$ and an error parameter ϵ , let a random*

variable C_i denote the number of keys in the $(i-1)$ -th level that a segment in the i -th level can cover (i.e., satisfying the error constraint ϵ). Specifically, C_0 denotes the leaf segment coverage (i.e., level-0) on the input key set \mathcal{K} . Then, the following recursion holds for $\mathbb{E}[C_i]$,

$$\mathbb{E}[C_i] = \frac{\mu^2 \cdot \epsilon^2}{\sigma^2} \cdot \mathbb{E}[C_0 \cdot C_1 \cdots C_{i-1}]. \quad (4)$$

PROOF. According to the law of total expectation [5],

$$\mathbb{E}[C_i] = \int \cdots \int \mathbb{E}[C_i | C_0 = c_0, \dots, C_{i-1} = c_{i-1}] \times f(c_0, \dots, c_{i-1}) dc_0 \cdots dc_{i-1}, \quad (5)$$

where $f(c_0, \dots, c_{i-1})$ is the joint probability density function of random variables C_0, \dots, C_{i-1} .

Suppose that g 's are the gaps of the original key set \mathcal{K} . When fixing C_0, \dots, C_{i-1} to c_0, \dots, c_{i-1} , as illustrated in Figure 4, w.l.o.g., an arbitrary gap in the i -th level, denoted by $g^{(i)}$, should be the sum of $c_0 \cdot c_1 \cdots c_{i-1}$ consecutive gaps on the raw key set \mathcal{K}^3 . Thus, according to Theorem 2.5, on a key set with gaps as $g^{(i)}$, the expected segment coverage (conditioned on C_0, \dots, C_{i-1}) in the i -th level for an ϵ -PLA should be,

$$\begin{aligned} \mathbb{E}[C_i | C_0 = c_0, \dots, C_{i-1} = c_{i-1}] &= \frac{\mathbb{E}[g^{(i)}]^2 \cdot \epsilon^2}{\text{Var}[g^{(i)}]} \\ &= \frac{\mathbb{E}\left[\sum_{j'=j}^{j+c_0 \cdot c_1 \cdots c_{i-1}} g_{j'}\right]^2 \cdot \epsilon^2}{\text{Var}\left[\sum_{j'=j}^{j+c_0 \cdot c_1 \cdots c_{i-1}} g_{j'}\right]} \\ &= (c_0 \cdot c_1 \cdots c_{i-1}) \cdot \frac{\mu^2 \cdot \epsilon^2}{\sigma^2}, \end{aligned} \quad (6)$$

where μ and σ^2 are the mean and variance of the gaps on the original key set \mathcal{K} . Taking Eq. (6) into the integral in Eq. (5), we have,

$$\begin{aligned} \mathbb{E}[C_i] &= \frac{\mu^2 \cdot \epsilon^2}{\sigma^2} \int \cdots \int \prod_{j=0}^{i-1} c_j \cdot f(c_0, \dots, c_{i-1}) dc_0 \cdots dc_{i-1} \\ &= \frac{\mu^2 \cdot \epsilon^2}{\sigma^2} \cdot \mathbb{E}[C_0 \cdot C_1 \cdots C_{i-1}]. \end{aligned} \quad (7)$$

Thus, we have the statement in Lemma 4.1. \square

LEMMA 4.2 (EXPECTED COVERAGE OF LEVEL- i). *The following lower bound holds for $\mathbb{E}[C_i]$,*

$$\mathbb{E}[C_i] \geq \left(\frac{\mu^2 \cdot \epsilon^2}{\sigma^2}\right)^{2^i}. \quad (8)$$

PROOF. We prove Lemma 4.2 using mathematical induction.

① **Base Case** ($i' = 0$): According to Theorem 2.5, $\mathbb{E}[C_0] = \mu^2 \epsilon^2 / \sigma^2$, satisfying the inequality in Eq. (8).

② **Inductive Step**: Assume that the lower bound in Eq. (8) holds for $i' = i-1$, i.e.,

$$\mathbb{E}[C_{i-1}] \geq \left(\frac{\mu^2 \cdot \epsilon^2}{\sigma^2}\right)^{2^{i-1}}. \quad (9)$$

Then, for the case of $i' = i$, according to Lemma 4.1, we have,

$$\begin{aligned} \mathbb{E}[C_i] &= \frac{\mu^2 \cdot \epsilon^2}{\sigma^2} \cdot \mathbb{E}[C_0 \cdot C_1 \cdots C_{i-1}] \\ &\geq \frac{\mu^2 \cdot \epsilon^2}{\sigma^2} \cdot \mathbb{E}[C_0 \cdot C_1 \cdots C_{i-2}] \cdot \mathbb{E}[C_{i-1}], \end{aligned} \quad (10)$$

³Here, we assume that all line segments within the same level exhibit equal coverage. A more rigorous analysis can be established by using concentration bounds like Chebyshev's inequality or Chernoff bound [5], which is omitted here for brevity.

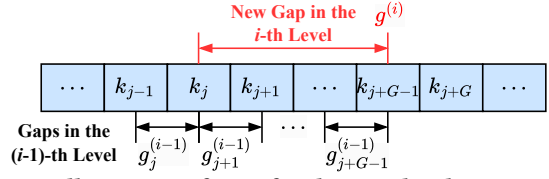


Figure 4: Illustration of gaps for the next level. Suppose G is the segment coverage for the current level. The new gap in the i -th level is $g^{(i)} = \sum_{j'=j+1}^{j+G-1} g_{j'}^{(i-1)}$ where $g_{j'}^{(i-1)}$ is the j' -th gap in the $(i-1)$ -th level.

considering that C_{i-1} is positively correlated with $C_0 \cdot C_1 \cdots C_{i-2}$. By the inductive hypothesis (i.e., Eq. (9)), we have,

$$\mathbb{E}[C_i] \geq \mathbb{E}[C_{i-1}]^2 \geq \left(\frac{\mu^2 \cdot \epsilon^2}{\sigma^2}\right)^{2^i}, \quad (11)$$

which satisfies the lower bound for $i' = i$. Thus, by induction, we conclude that Lemma 4.2 holds for all i . \square

THEOREM 4.3 (PGM-INDEX HEIGHT). *Given a set \mathcal{K} of N sorted keys, denote the constant $G = \mu^2 \epsilon^2 / \sigma^2$, w.h.p., the height of a PGM-Index with error parameter $\epsilon_i = \epsilon_\ell = \epsilon$ is bounded by*

$$H_{PGM} = O(\log_2 \log_G N) = O(\log \log N). \quad (12)$$

PROOF. Here we only provide an intuitive proof sketch due to the page limit. A more rigorous proof can be established by employing a similar technique as introduced in Theorem 4 of [10].

According to Definition 2.2, the construction of a PGM-Index terminates when the current level consists of exactly one line segment (i.e., reaching the root level). Intuitively, the index height H_{PGM} can be solved by letting

$$\frac{N}{\prod_{i=0}^{H_{PGM}-1} \mathbb{E}[C_i]} = O(1). \quad (13)$$

According to Theorem 4.2, we have,

$$\prod_{i=0}^{H_{PGM}-1} \mathbb{E}[C_i] \geq \prod_{i=0}^{H_{PGM}-1} G^{2^i} \geq G^{\sum_{i=0}^{H_{PGM}-1} 2^i} \geq G^{2^{H_{PGM}}}. \quad (14)$$

Thus, Eq. (13) can be solved by $H_{PGM} = O(\log_2 \log_G N)$. \square

THEOREM 4.4 (SPACE AND TIME COMPLEXITY). *Given a set \mathcal{K} of N sorted keys, a PGM-Index with $\epsilon_i = \epsilon_\ell = \epsilon$ can process an index lookup query in $O(\log \log N)$ time using $O(N/G)$ space.*

PROOF. According to Definition 2.2 and Example 2.3, querying a PGM-Index requires H_{PGM} times search operations, each within a range of $2 \cdot \epsilon + 1$. According to Theorem 4.3, the total index lookup time should be $O(H_{PGM} \cdot \log_2(2 \cdot \epsilon + 1)) = O(\log \log N)$.

We further analyze the space complexity of a PGM-Index, specifically the total number of line segments required to satisfy the error constraint ϵ . According to Definition 2.2 and Lemma 4.2, the h -th level contains at most $N / \prod_{i=0}^h G^{2^i}$ line segments. Thus, the upper bound on the total number of segments can be derived as,

$$\begin{aligned} \sum_{h=0}^{H_{PGM}-1} \frac{N}{\prod_{i=0}^h G^{2^i}} &\leq \sum_{h=0}^{H_{PGM}-1} \frac{N}{G^{h+1}} \leq N \cdot \frac{1 - \frac{1}{G^{H_{PGM}}}}{G-1} \\ &\leq \frac{N}{G-1} = O(N/G), \end{aligned} \quad (15)$$

considering that $\prod_{i=0}^h G^{2^i} \geq \prod_{i=0}^h G^{2^0} \geq G^{h+1}$. \square

Table 6: PGM-Index statistics on 10 million synthetic uniform keys with different ranges.

Key Range	ϵ	Height	Segments	Memory	\overline{Cov}
[0, 10 ⁸] $\mu = 10$ $\sigma^2 = 100.19$	4	4	129,503	2,078 KiB	77
	8	3	37,732	604 KiB	265
	16	3	10,224	163 KiB	978
	32	2	2,666	42 KiB	3,751
[0, 10 ⁹] $\mu = 100$ $\sigma^2 = 10007.7$	4	3	129,659	2,080 KiB	77
	8	3	37,601	602 KiB	266
	16	3	10,124	162 KiB	988
	32	2	2,665	42 KiB	3,752
[0, 10 ¹⁰] $\mu = 1000$ $\sigma^2 = 999750$	4	3	129,586	2,079 KiB	77
	8	3	37,597	602 KiB	266
	16	3	10,217	164 KiB	979
	32	2	2,646	42 KiB	3,779

4.3 Case Study: Uniform Keys

Previously, we assume that *gaps* are drawn from an *unknown* distribution. To further validate the correctness of our theoretical results, we now provide a case study on uniformly distributed *keys*.

Given a key set \mathcal{K} , assume that all keys $k \in \mathcal{K}$ are i.i.d. samples drawn from a uniform distribution $U(\alpha, \beta)$. In this case, the i -th gap on \mathcal{K} can be defined as $g_i = k_{(i)} - k_{(i-1)}$ where $k_{(i)}$ and $k_{(i-1)}$ are the i -th and $(i-1)$ -th order statistics of \mathcal{K} (i.e., the i -th and $(i-1)$ -th smallest values in \mathcal{K}). Then, for an arbitrary $i = 2, \dots, N$, it can be shown that g_i follows a beta distribution, $g_i \sim (\beta - \alpha) \cdot \text{Beta}(1, N)$, with the following mean and variance,

$$E[g_i] = \frac{\beta - \alpha}{N + 1}, \quad \text{Var}[g_i] = \frac{(\beta - \alpha)^2 \cdot N}{(N + 1)^2 \cdot (N + 2)} \approx \frac{(\beta - \alpha)^2}{(N + 1)^2}. \quad (16)$$

According to Eq. (16), the constant $G = \frac{\mu^2 \cdot \epsilon^2}{\sigma^2} = \epsilon^2$, which is interestingly independent of the original key distribution. By Theorem 2.4 and Theorem 4.4, this result implies that, for uniformly distributed keys, a PGM-Index should have the *same* index height and memory footprint as long as N and ϵ remain unchanged.

Table 6 reports the statistics for PGM-Indexes constructed on three synthetic uniform key sets with different ranges. The empirical results further validate the correctness of the aforementioned analysis, given that the index height and segment count remain consistent across different data ranges, depending solely on the value of error constraint ϵ .

Extension to Arbitrary Key Distributions. Suppose that the keys k_1, \dots, k_N are N i.i.d. random samples drawn from an *arbitrary* distribution with cumulative distribution function $F(x)$ and density function $f(x)$. As the i -th gap $g_i = k_{(i)} - k_{(i-1)}$, the distribution characteristics like mean and variance of g_i can be derived by evaluating the joint density function $f_{k_{(i-1)}, k_{(i)}}(x, y)$ of two consecutive order statistics $k_{(i-1)}$ and $k_{(i)}$ [5]. For example, the expectation $E[g_i]$ can be derived as,

$$E[g_i] = \iint (y - x) \cdot f_{k_{(i-1)}, k_{(i)}}(x, y) dx dy, \quad (17)$$

$$f_{k_{(i-1)}, k_{(i)}}(x, y) = \frac{N! \cdot F(x)^{i-2} (1 - F(y))^{N-i} f(x) f(y)}{(i-2)!(N-i)!}.$$

Notably, in most cases, no closed-form solution exists for Eq. (17). Thus, an empirical CDF (ECDF) based on random sampling can be applied to obtain a provably accurate approximation according to the DKW bound [9].

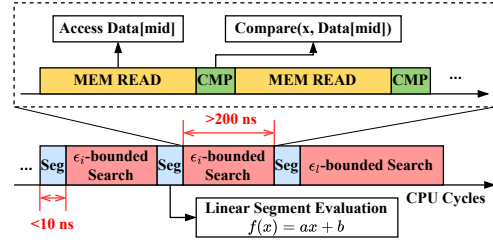


Figure 5: Illustration of the CPU cycles used for searching an (ϵ_i, ϵ_l) -PGM-Index with a standard binary search algorithm for the internal error-bounded search operation.

5 WHY ARE PGM-INDEXES INEFFECTIVE?

The theoretical findings in Section 4 reveal that PGM-Indexes can achieve the best space-time trade-off among existing learned indexes. However, according to recent benchmarks [22, 44], an optimized RMI [18] consistently outperforms the PGM-Index by 20%–40%. Motivated by this, in this section, we aim to answer another critical question: Why do PGM-Indexes underperform in practice?

A Simple Cost Model. We begin by introducing a simplified cost model for an arbitrary (ϵ_i, ϵ_l) -PGM-Index. Recalling the PGM-Index structure as shown in Figure 2, the total index lookup time for a search key k can be modeled as the summation of the internal search cost with error constraint ϵ_i and the last-mile search cost with error constraint ϵ_l , i.e.,

$$\text{Cost} = \text{Cost}_{\text{internal}} + \text{Cost}_{\text{last-mile}} \quad (18)$$

$$= (H_{PGM} - 1) \cdot C_S(\epsilon_i) + C_S(\epsilon_l) + H_{PGM} \cdot C_L,$$

where H_{PGM} is the index height, $C_S(\epsilon)$ represents the search cost within the range of $2 \cdot \epsilon + 1$, and C_L is the overhead to evaluate a linear function $y = a \cdot x + b$.

Bottleneck: Error-bounded Search. According to Theorem 2.4, the index height $H_{PGM} = O(\log \log N)$, implying that very few internal searches are required (generally fewer than 5 for 1 billion keys). Additionally, as depicted in Figure 5, our benchmark results across various datasets and platforms indicate that evaluating a linear function typically takes **less than 10 ns**. In contrast, performing a search with $\epsilon = 64$ takes time **more than 200 ns** by adopting a standard binary search implementation (e.g., `std::lower_bound`). Based on this observation, the cost model in Eq. (18) can be simplified by neglecting the segment evaluation overhead, i.e.,

$$\text{Cost} \approx (H_{PGM} - 1) \cdot C_S(\epsilon_i) + C_S(\epsilon_l). \quad (19)$$

The revised cost model reveals that searching a PGM-Index is dominated by performing H_{PGM} times error-bounded searches, which are generally known as *memory-bound* operations [43]. As depicted in Figure 5, an ϵ -bounded binary search typically involves $\lceil \log_2(2 \cdot \epsilon + 1) \rceil$ comparisons and memory accesses. Each comparison generally requires a few nanoseconds, whereas each memory access, if cache missed, can take approximately 100 nanoseconds due to the asymmetric nature of the memory hierarchy.

Comparison to RMI. We then investigate why RMI practically outperforms the PGM-Index. As illustrated in Figure 6, the major structural difference between RMI and PGM-Index lies in their internal search mechanisms. For RMI, the model prediction $f_{i,j}(k)$ directly serves as the *model index* for the next level (i.e., the $(i+1)$ -th level), thereby bypassing the costly internal error-bounded search used in PGM-Index. To ensure lookup correctness, the models in

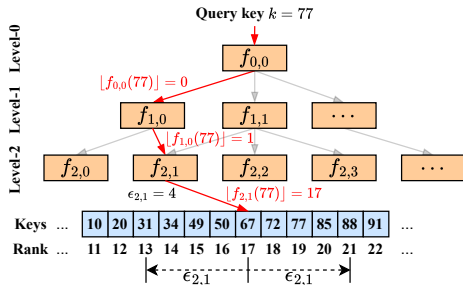


Figure 6: Illustration of a 3-layer RMI [18]. $f_{i,j}$ denotes the j -th model in the i -th layer. The path in red denotes the index traversal from the root model $f_{0,0}$. Notably, the root level is specified as level-0, opposite to the PGM-Index.

the bottom layer materialize the *maximum search error* to perform a last-mile error-bounded search, similar to the PGM-Index.

Table 7 presents the detailed overheads when querying RMI and PGM-Index. Consistent with previous benchmark results [22], an optimized RMI implementation [32] outperforms the PGM-Index in terms of total index lookup time across all datasets. Specifically, for PGM-Index, the internal search time T_i accounts for **69%–81%** of the total index lookup overhead; in contrast, for RMI, this ratio is as low as **19%–27%**, supporting our earlier claim.

Is RMI the Best Choice? While RMI generally outperforms the PGM-Index, its design poses a critical limitation: RMI is hard to guarantee a maximum error before index construction, making its performance highly *data-sensitive*. As shown in Table 7, RMI’s maximum error ranges from **63** to 3.1×10^5 , resulting in high *worst-case* last-mile search overhead. Such “unpredictability” also raises the challenge of building an accurate cost model for RMI-like indexes, which is crucial for practical DBMS to perform effective cost-based query optimization [13]. Moreover, given the identified bottleneck in querying a PGM-Index, a natural idea is to accelerate the costly internal error-bounded search operation. In Section 6, we demonstrate how a simple hybrid branchless search strategy can make the “ineffective” PGM-Index outperform RMI.

6 PGM++: OPTIMIZATION TO PGM-INDEX

This section introduces PGM++, a *simple yet effective* variant of the PGM-Index by incorporating a hybrid error-bounded search strategy (\triangleright Section 6.1) and an automatic parameter tuner based on well-calibrated cost models (\triangleright Section 6.2).

6.1 Hybrid Search Strategy

As the error-bounded search operation is identified as the bottleneck in querying the PGM-Index, our optimized structure, named PGM++, employs a *hybrid search strategy* to replace the standard binary search. To start, we discuss the impact of branch misses in standard binary search implementation.

Branch Prediction and Branch Miss. Modern CPUs rely on sophisticated branch predictors to enhance pipeline parallelism by forecasting the outcomes of conditional jump instructions (e.g., JLE and JAE instructions in the X86 architecture). These predictors are highly effective for simple, repetitive tasks such as for loops or pointer chasing, where the pattern of execution is predictable [12]. However, in the case of standard binary search implementations, such as the widely used `std::lower_bound`, branching exhibits a

Table 7: Query processing details. For PGM-Index, $\epsilon_i = 16$ and $\epsilon_l = 32$. For RMI, we adopt CDFShop [24] to find an optimized RMI structure with a comparable space to the PGM-Index.

Data	Index	Size	Max Err.	Internal Time	Last-mile Time	Total
fb	PGM	16.1 MB	32	675 ns	300 ns	975 ns
	RMI	24.0 MB	568	185 ns	614 ns	799 ns
wiki	PGM	1.3 MB	32	606 ns	270 ns	876 ns
	RMI	1.0 MB	63	95 ns	317 ns	412 ns
books	PGM	37.6 MB	32	887 ns	208 ns	1095 ns
	RMI	40.0 MB	302	159 ns	429 ns	588 ns
osm	PGM	44.4 MB	32	824 ns	212 ns	1036 ns
	RMI	96.0 MB	311K	146 ns	636 ns	782 ns

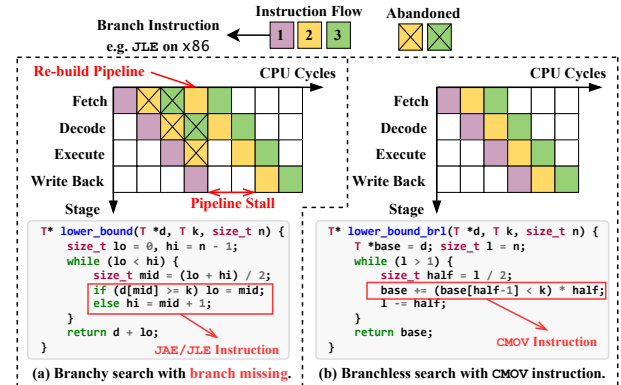


Figure 7: Illustration of the CPU pipeline status for executing (a) standard binary search (`std::lower_bound`) and (b) branchless binary search enabled by CMOV instruction.

random pattern, leading to a high branch miss rate of approximately **50%** [34]. As depicted in Figure 7(a), a branch miss stalls the entire CPU pipeline until the branch condition is resolved (e.g., the comparison $d[\text{mid}] \geq k$ in line 5 of function `lower_bound`).

Branchless Binary Search. A simple optimization [34] to the standard binary search is to *remove* the branches by conditional move instructions (e.g., CMOV on X86 and MOVGE on ARM), which allow *both* sides of a branch to execute and keeps the valid one based on the evaluated condition. As illustrated in Figure 7(b), eliminating branches (function `lower_bound_br1`) maximizes the CPU pipeline utilization, yielding up to a **51%** reduction in total search time. Notably, CMOV is not the “silver bullet” as it disables the native branch predictor and incurs extra overhead due to its intrinsic complexity. On large datasets ($> \text{LLC size}$), the performance gap between branchy and branchless searches diminishes as the memory access latency dominates the total overhead. However, such extra overhead is *negligible* particularly when the search range fits within the L2 cache, making CMOV performance-worthy in PGM-Index (usually $\epsilon \leq 1024$).

Benchmark Results. Figure 8 presents the benchmark result for branchy binary search (`std::lower_bound` from STL), branchless binary search (similar to `lower_bound_br1` in Figure 7(b)), and linear scan, tested on synthetic `uint64_t` key sets of varying sizes. The results indicate that, on both ARM and X86 platforms, branchless search demonstrates superior performance across a wide range of data sizes, excluding very small sets (e.g., $N \leq 16$), where the

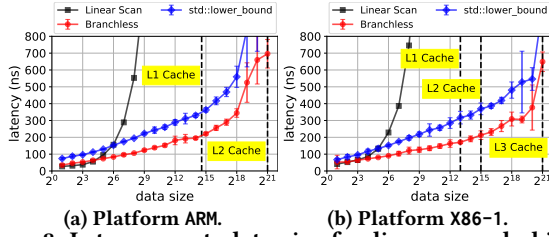


Figure 8: Latency w.r.t. data size for linear search, binary search (`std::lower_bound`), and branchless binary search.

linear scan is more efficient. Compared to `std::lower_bound`, our branchless search implementation achieves a performance improvement of approximately 1.2× to 1.6×.

It is noteworthy that other search algorithms, like k-ary search and interpolation search [34], are not included in this comparison. This is because, the search range in the PGM-Index is typically small (e.g., $\epsilon \leq 1024$), where more advanced search algorithms do not consistently outperform a branchless binary search. Additionally, we do not consider architecture-aware optimizations like SIMD and memory pre-fetching, as our work is intended to provide a detailed theoretical and experimental revisit of the original PGM-Index [11]. The simple hybrid search strategy, as described below, is sufficient to showcase the potential of PGM-Index.

Hybrid Search. Based on the above discussion and benchmark results, our PGM++ adopts the following *hybrid search* operator:

$$\text{hybrid_search} = \begin{cases} \text{linear_scan} & \text{if Search Range} \leq \delta \\ \text{lower_bound_brl} & \text{if Search Range} > \delta \end{cases}$$

where δ is a threshold to switch to linear search (8 on ARM/X86-1, and 16 on X86-2). Then, as illustrated in Figure 9, PGM++ processes an index lookup query as follows. **Step ①:** Starting from the root layer, identify the layer l where the *next* layer’s segment count exceeds δ and skip all the layers before l . **Step ②:** Starting from layer l , perform internal searches (using `hybrid_search`) with error bound ϵ_i until reaching the bottom layer. **Step ③:** Perform last-mile search on sorted keys (using `hybrid_search`) with error bound ϵ_ℓ . Notably, the specific search strategy for each layer can be determined at compile time, without introducing any extra runtime overhead.

Recalling our theoretical findings in Section 4, the height of PGM-Index grows at a sub-logarithmic rate of $O(\log \log N)$, leading to an extremely *flat* hierarchical structure where the *non-bottom* layers contain very few line segments. Due to the structural invariance of PGM-Index (as defined in Definition 2.2), instead of recursively searching from the root, PGM++ skips all layers until reaching the first layer whose next layer is considered *dense* (segment count $> \delta$). This strategy, outlined in Step ①, effectively reduces search overhead, particularly in a *cold-cache* environment.

6.2 Calibrated Cost Model

To efficiently and effectively determine the error bounds for internal search (ϵ_i) and last-mile search (ϵ_ℓ), we first develop cost models that estimate the space and time overheads without the need for physically constructing the PGM-Index.

Space Cost Model. According to Section 4.1 and Table 5, the space overhead of a PGM-Index is predominantly determined by the number of segments in the bottom layer (denoted as L), which accounts for up to > 99.9% of the total space cost. Therefore, to

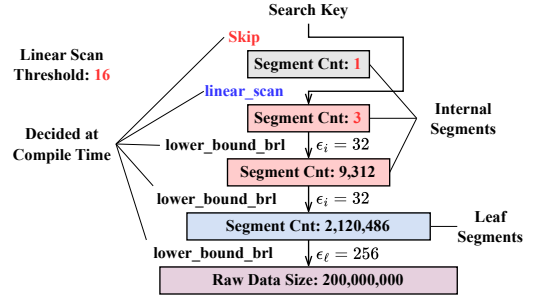


Figure 9: A toy example of the hybrid search strategy.

simplify the space cost model, we focus solely on the leaf segments and ignore the internal segments. According to the results in [10] (i.e., Theorem 2.5), $L \propto N\sigma^2/\epsilon_\ell^2\mu^2$, where μ and σ^2 refer to the mean and variance of *gaps* on the input sorted keys, respectively.

However, as discussed in Section 3, this estimation, which relies on the *global* gap distribution, is often too *coarse* for practical datasets due to the inherent heterogeneity in gap distributions. To develop a more fine-grained cost model, we partition the gaps into a set of consecutive and disjoint chunks \mathcal{P} (with $\sum_{P \in \mathcal{P}} |P| = N$) by using a kernel-based change-point detection algorithm [2]. Assuming that gaps are identically distributed within each partition $P \in \mathcal{P}$, the refined estimator for L becomes:

$$L(\epsilon_\ell) \propto \sum_{P \in \mathcal{P}} N_P \sigma_P^2 / \epsilon_\ell^2 \mu_P^2, \quad (20)$$

where N_P , μ_P , and σ_P^2 represent the size, mean, and variance of gaps within partition $P \in \mathcal{P}$, respectively. The total space cost of an $(\epsilon_i, \epsilon_\ell)$ -PGM-Index is then given by $M = L(\epsilon_\ell) \cdot \text{sizeof}(seg)$, where $\text{sizeof}(seg)$ is the number of bytes required to encode a line segment $seg = (s, a, b)$. Typically, $\text{sizeof}(seg) = 24$ for `uint64_t` keys and `double` slope and intercept.

Time Cost Model. According to the discussions in Section 5, the majority of the index lookup overhead comes from the recursively invoked error-bounded search operations. As we adopt a hybrid search strategy, the simplified cost model introduced in Eq. (19) can be further refined as follows,

$$\text{Cost}(\epsilon_i, \epsilon_\ell) = \text{Cost}_{\text{internal}} + \text{Cost}_{\text{last-mile}} \quad (21a)$$

$$\text{Cost}_{\text{last-mile}} = \lceil \log_2(2 \cdot \epsilon_\ell + 1) \rceil \cdot C_{\text{miss}} \quad (21b)$$

$$\text{Cost}_{\text{internal}} = (H_{\text{PGM}} - 1) \cdot (C_S(\epsilon_i) + C_{\text{segment}}) \quad (21c)$$

$$C_S(\epsilon_i) = \begin{cases} C_{\text{linear}} & \text{if } 2 \cdot \epsilon_i + 1 \leq \delta \\ \lceil \log_2(2 \cdot \epsilon_i + 1) \rceil \cdot C_{\text{hit}} & \text{if } 2 \cdot \epsilon_i + 1 > \delta \end{cases} \quad (21d)$$

$$H_{\text{PGM}} \propto \log_2 \log_{\mu^2 \epsilon_i^2 / \sigma^2} L(\epsilon_\ell) \quad (21e)$$

where (a) constants C_{miss} and $C_{\text{last-mile}}$ are the memory access costs when missing or hitting L1/L2 cache; (b) constant C_{segment} refers to the overhead of evaluating a linear function $y = a \cdot x + b$; (c) constant C_{linear} is the cost of performing a linear search within the range of $2 \cdot \epsilon_i + 1$; and (d) $L(\epsilon_\ell)$ is the count of leaf segments estimated by Eq. (20). Notably, all constants in the cost model are estimated by probe datasets for each platform.

In Eq. (21b), we assume a *cold-cache* environment, as the raw key set \mathcal{K} is large enough and the access to \mathcal{K} is too random for hardware prefetchers to be effective. Conversely, in Eq. (21d), we assume a *hot-cache* environment, since the non-bottom layers contain very few segments, making it highly likely for these segments to be cache-resident after processing a few queries. It is noteworthy that

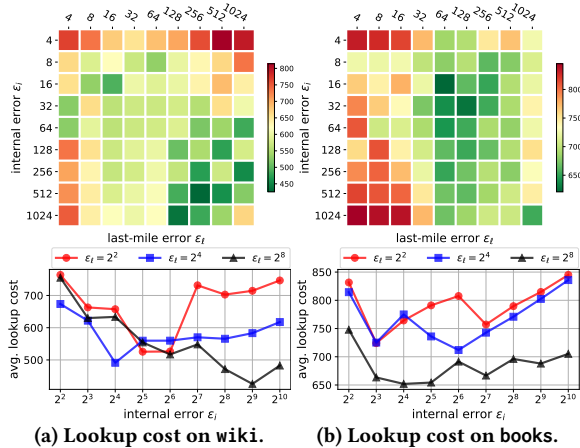


Figure 10: Observed index lookup overhead (unit: ns) of PGM++ on x86-1 w.r.t. different combinations of (ϵ_i, ϵ_l) .

when index data can be well-cached by the CPU, the segment computation overhead becomes non-negligible. That is why Eq. (21c) includes an additional term C_{segment} .

PGM-Index Parameter Tuning. With the space and time cost models, the two error parameters, ϵ_i and ϵ_l , can be automatically configured by minimizing the potential lookup cost while satisfying a pre-specified space constraint. **Step 1:** Given a *rough* index storage budget B , according to Eq. (20), ϵ_l can be estimated by

$$\tilde{\epsilon}_l = \sqrt{\frac{\text{sizeof}(\text{seg})}{B} \sum_{P \in \mathcal{P}} N_P \sigma_P^2 / \mu_P^2}. \quad (22)$$

Step 2: With a determined $\epsilon_l = \tilde{\epsilon}_l$, ϵ_i can be derived by minimizing the index search overhead as formulated in Eq. (21a), i.e.,

$$\tilde{\epsilon}_i = \arg \min_{\epsilon_i \in \mathcal{E}} \text{Cost}(\epsilon_i, \tilde{\epsilon}_l), \quad (23)$$

where \mathcal{E} is the set of possible values for ϵ_i ($\mathcal{E} = \{2^j | j = 2, \dots, 10\}$ in our implementation). Intuitively, to minimize Eq. (21a), ϵ_i should neither be too large nor too small. According to the cost model, a larger ϵ_i increases the overhead of $C_S(\epsilon_i)$ in Eq. (21d), while a smaller ϵ_i results in more layers to traverse (i.e., H_{PGM} in Eq. (21e)). Notably, although Eq. (23) has an analytical solution by solving $\frac{\partial \text{Cost}}{\partial \epsilon_i} = 0$, in practice, we simply enumerate all possible $\epsilon_i \in \mathcal{E}$ to find the optimal value, as \mathcal{E} is typically a small set ($|\mathcal{E}| < 10$).

Figure 10 reports the results of the observed index lookup costs w.r.t. different values of ϵ_i and ϵ_l . When fixing ϵ_l , the time cost w.r.t. ϵ_i exhibits a “U”-shaped pattern, consistent with our earlier analysis based on the established cost model.

Takeaways. Our cost model for PGM++ can be easily extended to *any* PGM-Index variants like [11, 52]. In contrast to existing cost models for learned indexes (mostly based on RMI) like [50], our cost model is *workload-independent*, relying solely on gap distribution characteristics and platform-aware cost constants. These features enhance the robustness of parameter tuning, as the cost is optimized for *all* queries rather than being tailored to a specific workload.

7 EXPERIMENTAL STUDY

In this section, we present the major benchmark results to answer the vital question that whether PGM++ is capable of reversing the “ineffective” scenario of PGM-Indexes. The experimental setups have been detailed in Section 3.

7.1 Overall Evaluation

Baseline and Implementation. We implement and evaluate three learned indexes: 1 RMI, the optimized recursive model index [18, 22], 2 PGM, the original PGM-Index implementation [11, 29], and 3 PGM++, our optimized PGM-Index variant. For RMI, we adopt CDFShop [24] to produce a set of optimal RMI configurations under various index sizes. For PGM, we construct 9×9 PGM-Indexes with $(\epsilon_i, \epsilon_l) \in \mathcal{E} \times \mathcal{E}$ and $\mathcal{E} = \{2^2, \dots, 2^{10}\}$. Then, for each $\epsilon_l \in \mathcal{E}$, the fastest PGM-Index is reported. Similarly, for PGM++, we adopt the PGM-Index configuration tuned by cost models (Section 6.2) for each $\epsilon_l \in \mathcal{E}$. For PGM and PGM++, according to Eq. (20), each ϵ_l corresponds to an index storage budget.

We do not consider other PGM or RMI variants, such as the cache-efficient RMI [50] or the IO-efficient PGM-Index [52]. This is because this work *primarily* aims at exploring the theoretical aspect and performance bottlenecks inherent in the PGM-Index. Our findings, however, possess a broader applicability, as they can be generalized to *any* PGM-like indexes. This study also excludes non-learned baselines like B+-tree variants as they have been extensively compared in previous learned index benchmarks like [22, 44]. **Overall Evaluation.** Figure 11 presents the trade-offs between index lookup overhead and storage cost across all seven datasets and three platforms on Uniform query workloads. The results show that, in terms of index lookup time, PGM++ consistently outperforms PGM by a factor of $1.2\times \sim 2.2\times$ with the same index size, supporting our bottleneck analysis for PGM-Indexes (Section 5). In contrast to the optimized RMI, our PGM++ addresses the costly internal index traversal through a hybrid search strategy, generally delivering better or, in some cases, comparable lookup efficiency, achieving speedups of up to $1.56\times$. An outlier case is on dataset normal, RMI significantly outperforms PGM++ and PGM. The reason is that the optimized RMI, based on CDFShop [24], adopts non-linear models (with the best RMI uses cubic splines), which can fit normal keys very well (maximum error < 4). However, on other datasets, especially complex real-world datasets, RMI fell short in fitting the data with constrained error limits, leading to costly last-mile search overhead as discussed in Section 5.

Space-time Trade-off. In most cases, PGM++ offers the best space-time trade-off. However, interestingly, unlike RMI, whose performance improves with increased index memory usage, PGM++ exhibits an “irregular” pattern in its time-space relationship. This is because PGM++ is specifically optimized for query efficiency at a given storage budget. Leveraging accurate cost models, our parameter tuner can find configurations to provide competitive query efficiency, even under limited space constraints. For example, on dataset wiki, PGM++ uses just 0.1 MB of memory to outperform an RMI with over 100 MB space.

Influence of Architecture. From Figure 11, the comparison results vary across different platforms. For dataset osm, compared to PGM, PGM++ achieves an average speedup ratio of $1.78\times$ on x86-1 and arm. However, such a speedup decreases to $1.32\times$ on platform x86-2. This is because the memory access latency on x86-2 is much higher than that on x86-1, which reduces the improvement brought by adopting the hybrid search strategy.

Effects of Workloads. We also evaluate an extreme query workload, Zipfan, though the results are not included in this paper due

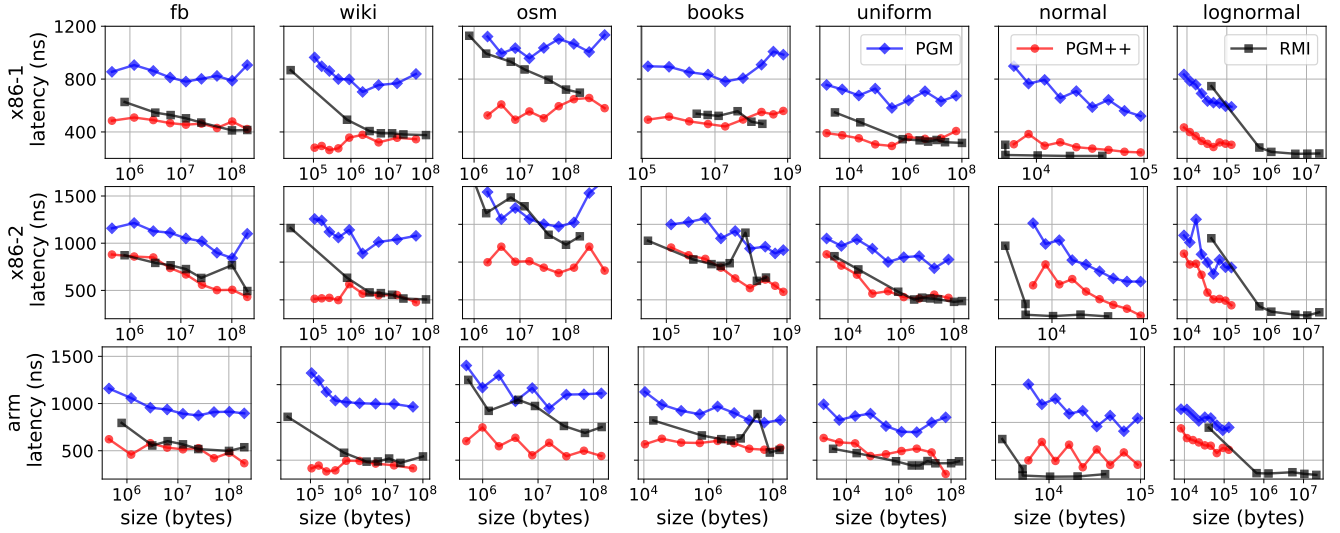


Figure 11: Space and time tradeoffs for seven datasets on three platforms (workload: Uniform).

to space limits. Queries sampled from a Zipfan distribution exhibit a highly *long-tail* pattern, where the first 1K elements are frequently accessed (Section 3). Under this workload, PGM++, PGM, and RMI all achieve lower query latencies by up to 1.77 \times , 2.13 \times , and 4.58 \times , respectively, compared to their performance on Uniform workloads. RMI shows the most substantial gains, as the last-mile search cost dominates the total index lookup time (> 90%). This phase benefits greatly from the spatial locality inherent in the Zipfan workload, where frequently accessed memory is more likely to be cached.

7.2 Cost Model and Parameter Tuner

Space Cost Model. According to Section 6.2, the leaf segment count (L) dominates the PGM-Index space cost. Here, we evaluate three different segment count estimators: (a) SIMPLE, which directly applies Theorem 2.5 on the *entire* gap distribution; (b) CLIP, which applies Theorem 2.5 on the gaps excluding extreme values (<0.01-quantile or >0.99-quantile); and (c) ADAP, which partitions gaps into disjoint chunks and aggregates the segment count estimated for each chunk (as in Eq. (20)).

As shown in Figure 12, compared to the true segment count (TRUE), ADAP consistently achieves accurate estimations across all seven datasets, nearly overlapping the TRUE line. In addition, excluding uniformly distributed datasets (e.g., books and uniform), SIMPLE performs the worst, validating our discussion in Section 3 that extreme gap values significantly affect estimation accuracy. Notably, CLIP also delivers accurate results on real datasets fb, wiki, and osm. This is because, on these datasets, the gaps are *nearly* identically distributed after removing the extreme values, thus better satisfying the requirement of using Theorem 2.5.

Time Cost Model. For each pair of $(\epsilon_i, \epsilon_\ell) \in \mathcal{E} \times \mathcal{E}$, where $\mathcal{E} = \{2^j \mid j = 2, 3, \dots, 10\}$, we estimate the index lookup overhead as $Cost(\epsilon_i, \epsilon_\ell)$ using the time cost model (i.e., Eq. (21a)–Eq. (21e)), and then physically construct the corresponding $(\epsilon_i, \epsilon_\ell)$ -PGM-Index to measure the actual lookup time (averaged over a given workload).

Figure 13 visualizes the relationship between the true index lookup overhead and the cost model’s estimation. The closer the points in Figure 13 are to the line $y = x$, the more accurate the

estimation. From the results, our cost model closely approximates the true index lookup overhead, especially for the three synthetic datasets uniform, normal, and lognormal. This is because synthetic datasets strictly follow i.i.d. gaps assumptions, leading to more precise estimates of the index height (Eq. (21e)), which significantly affects the total time cost estimation (Eq. (21c)).

Parameter Tuning Strategy. We finally evaluate PGM++’s parameter tuner as introduced in Section 6.2. For a given ϵ_ℓ , which is directly solved given a pre-specified storage budget (Eq. (22)), we record the index lookup overhead for PGM-Indexes with different ϵ_i configurations: (a) T_{PGM++} , where ϵ_i is automatically tuned using our cost model, (b) T_{rand} , where ϵ_i is randomly selected, and (c) T_{opt} , which is the optimal time cost by testing all possible ϵ_i values.

Figure 14 reports the *relative* index lookup overhead w.r.t. different ϵ_ℓ settings (i.e., $T_{PGM++}/T_{opt} - 1$ and $T_{rand}/T_{opt} - 1$). From the results, across all datasets and ϵ_ℓ settings (i.e., storage budgets), PGM++’s automatic parameter tuning strategy consistently finds a better ϵ_i to reduce the index lookup overhead. Specifically, in 46% of cases, PGM++ successfully picks the **optimal** ϵ_i , and in 91% of cases, PGM++ finds a configuration that is only < 10% worse than the optimal one in terms of actual index lookup overhead.

Takeaways. The experimental results reveal that in over 90% of cases, PGM++’s parameter tuner identifies a **near-optimal** index configuration, introducing less than 10% extra index lookup overhead. In addition, our parameter tuner is much more efficient than CDFShop [24] designed for optimizing RMI structures (requiring <1 μ s v.s. >10 minutes). This is because instead of physically constructing the index, our method only depends on gap distribution characteristics, which can be pre-computed and re-used.

8 RELATED WORK

Learned Indexes. Indexing one-dimensional sorted keys has been a well-explored topic for decades. While mainstream tree-based indexes (e.g., B+-tree [6], FAST [14], ART [4], Wormhole [47], HOT [4], etc.) are widely adopted in commercial DBMS, a new class of data structure, known as *learned index*, has recently gained significant attention in both academia and industry [8, 11, 18, 36,

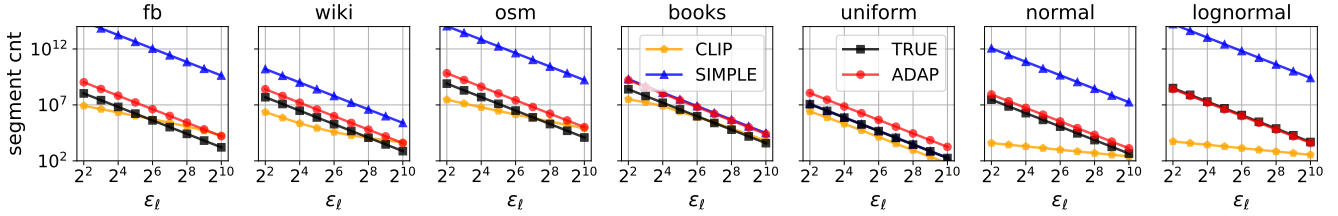


Figure 12: Evaluation of the space cost model (Eq. (20)). For each ϵ_ℓ , we compare three leaf segment count estimators: (a) SIMPLE, (b) CLIP, and (c) ADAP. TRUE refers to the actual observed leaf segment count.

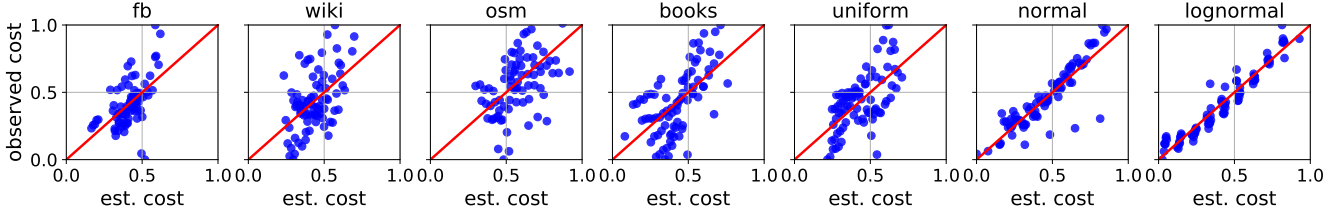


Figure 13: Evaluation of the time cost model (Eq. (21a)–Eq. (21e)). We plot the true index lookup costs (normalized) against the estimated costs (normalized) on platform x86-1, where each point corresponds to a unique pair of $(\epsilon_i, \epsilon_\ell)$ configuration.

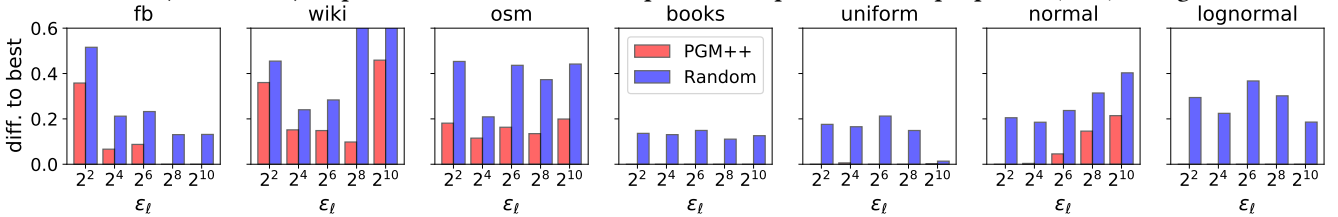


Figure 14: Evaluation of parameter tuning. The y-axis is the relative difference compared to the optimal configuration when fixing ϵ_ℓ . Red bars and blue bars refer to the ϵ_i settings selected by using PGM++’s cost model and randomly picking, respectively.

40, 45, 46, 50, 52, 53]. Intuitively, learned indexes directly fit the CDF over sorted keys with controllable error to perform an error-bounded last-mile search. By properly organizing the model structure, learned indexes offer the potential for superior space-time trade-offs compared to conventional tree-based indexes [22, 44].

Existing learned indexes can be roughly categorized as either RMI-like [18] or PGM-like [11], based on whether the error-bounded search occurs during the index traversal phase. This work delves deeply into the theoretical and empirical aspects of the PGM-Index, highlighting its potential to be *practically* embedded into real DBMS. **Learned Index Theories.** Unlike tree-based indexes, which are supported by well-established theoretical foundations, the effectiveness of learned indexes has largely been demonstrated through *empirical results*. Ferragina et al. [10, 11] first prove that the expected time and space complexities of a PGM-Index with error constraint ϵ on N keys should be $O(\log N)$ and $O(N/\epsilon^2)$, respectively. In parallel, another recent work [49] focuses on an RMI variant with *piece-wise constant* models, achieving an index lookup time of $O(\log \log N)$ but using *super-linear* space of $O(N \log N)$.

In this work, we tighten the results of [10] by achieving a sub-logarithmic time complexity of $O(\log \log N)$ while maintaining *linear* space, $O(N/\epsilon^2)$, for PGM-Indexes. To the best of our knowledge, this is the tightest bound among all existing learned indexes. **Learned Index Cost Model.** Modeling the space and time overheads of an index structure is crucial for both index parameter configuration and DBMS query optimization. Existing learned indexes mainly adopt a workload-based cost model, which assumes prior knowledge of the query distribution [24, 50]. In contrast, by extending the theoretical results, we establish a cost model for

PGM-like indexes without *any* assumptions on query workloads. As our cost model is simple, parameter tuning based on it is much more efficient than workload-driven approaches, making it more feasible to be integrated into practical DBMS.

AI4DB. Beyond learned indexing, recent advancements in AI are reshaping traditional approaches on decades-old data management challenges, such as query planning [23, 48, 54], cardinality estimation [16, 39], approximate query processing [20, 38], SQL generation [15, 41], DBMS configuration [1, 51], etc.

9 CONCLUSION AND FUTURE WORK

This work provides a thorough theoretical and experimental revisit to the PGM-Index. We establish a new bound for the PGM-Index by showing the $O(\log \log N)$ index lookup time while using $O(N/G)$ space. We further identify that costly internal error-bounded search operations have become a bottleneck in practice. Based on such findings, we propose PGM++, a simple yet effective PGM-Index variant, by improving the internal search subroutine and configuring index hyper-parameters based on accurate cost models. Extensive experimental results demonstrate that PGM++ speeds up index lookup queries by up to 2.31 \times and 1.56 \times compared to the original PGM-Index and the optimized RMI implementation, respectively.

Future Work. ① Our theoretical results inherit the i.i.d. assumption on *gaps* from previous analyses. In our future work, we aim to relax this assumption to demonstrate that the sub-logarithmic bound still holds for weakly correlated data. ② To further accelerate PGM++, we plan to fully exploit architecture-aware optimizations like memory pre-fetching and SIMD. Additionally, we will release a GPU-accelerated version of PGM++.

REFERENCES

- [1] Dana Van Aken, Andrew Pavlo, Geoffrey J. Gordon, and Bohan Zhang. 2017. Automatic Database Management System Tuning Through Large-scale Machine Learning. In *SIGMOD Conference*. ACM, 1009–1024.
- [2] Sylvain Arlot, Alain Celisse, and Zaïd Harchaoui. 2019. A Kernel Multiple Change-point Algorithm via Model Selection. *J. Mach. Learn. Res.* 20 (2019), 162:1–162:56.
- [3] biglittle [n.d.]. big.LITTLE: Balancing Power Efficiency and Performance. <https://www.arm.com/en/technologies/big-little>. Accessed: 2024-06-12.
- [4] Robert Binna, Eva Zangerle, Martin Pichl, Günther Specht, and Viktor Leis. 2018. HOT: A Height Optimized Trie Index for Main-Memory Database Systems. In *SIGMOD Conference*. ACM, 521–534.
- [5] Kai Lai Chung. 2000. *A course in probability theory*. Elsevier.
- [6] Douglas Comer. 1979. The Ubiquitous B-Tree. *ACM Comput. Surv.* 11, 2 (1979), 121–137.
- [7] Thomas H Cormen, Charles E Leiserson, Ronald L Rivest, and Clifford Stein. 2022. *Introduction to algorithms*. MIT press.
- [8] Jialin Ding, Umar Farooq Minhas, Jia Yu, Chi Wang, Jaeyoung Do, Yinan Li, Hantian Zhang, Badrish Chandramouli, Johannes Gehrke, Donald Kossmann, David B. Lomet, and Tim Kraska. 2020. ALEX: An Updatable Adaptive Learned Index. In *SIGMOD Conference*. ACM, 969–984.
- [9] Aryeh Dvoretzky, Jack Kiefer, and Jacob Wolfowitz. 1956. Asymptotic minimax character of the sample distribution function and of the classical multinomial estimator. *The Annals of Mathematical Statistics* (1956), 642–669.
- [10] Paolo Ferragina, Fabrizio Lillo, and Giorgio Vinciguerra. 2020. Why Are Learned Indexes So Effective?. In *ICML (Proceedings of Machine Learning Research)*, Vol. 119. PMLR, 3123–3132.
- [11] Paolo Ferragina and Giorgio Vinciguerra. 2020. The PGM-index: a fully-dynamic compressed learned index with provable worst-case bounds. *Proc. VLDB Endow.* 13, 8 (2020), 1162–1175.
- [12] John L Hennessy and David A Patterson. 2011. *Computer architecture: a quantitative approach*. Elsevier.
- [13] Matthias Jarke and Jürgen Koch. 1984. Query Optimization in Database Systems. *ACM Comput. Surv.* 16, 2 (1984), 111–152.
- [14] Changkyu Kim, Jatin Chhugani, Nadathur Satish, Eric Sedlar, Anthony D. Nguyen, Tim Kaldewey, Victor W. Lee, Scott A. Brandt, and Pradeep Dubey. 2010. FAST: fast architecture sensitive tree search on modern CPUs and GPUs. In *SIGMOD Conference*. ACM, 339–350.
- [15] Hyeonji Kim, Byeong-Hoon So, Wook-Shin Han, and Hongrae Lee. 2020. Natural language to SQL: Where are we today? *Proc. VLDB Endow.* 13, 10 (2020), 1737–1750.
- [16] Andreas Kipf, Thomas Kipf, Bernhard Radke, Viktor Leis, Peter A. Boncz, and Alfons Kemper. 2019. Learned Cardinalities: Estimating Correlated Joins with Deep Learning. In *CIDR*. www.cidrdb.org.
- [17] Andreas Kipf, Ryan Marcus, Alexander van Renen, Mihail Stoian, Alfons Kemper, Tim Kraska, and Thomas Neumann. 2020. RadixSpline: a single-pass learned index. In *aiDM@SIGMOD*. ACM, 5:1–5:5.
- [18] Tim Kraska, Alex Beutel, Ed H. Chi, Jeffrey Dean, and Neoklis Polyzotis. 2018. The Case for Learned Index Structures. In *SIGMOD Conference*. ACM, 489–504.
- [19] Justin J. Levandoski, David B. Lomet, and Sudipta Sengupta. 2013. The Bw-Tree: A B-tree for new hardware platforms. In *ICDE*. IEEE Computer Society, 302–313.
- [20] Qingzhi Ma, Ali Mohammadi Shanghooshabad, Mehrdad Almasi, Meghdad Kurmanji, and Peter Triantafyllou. 2021. Learned Approximate Query Processing: Make it Light, Accurate and Fast. In *CIDR*. www.cidrdb.org.
- [21] macbook2024 [n.d.]. MacBook Air (13-inch, M3, 2024) - Technical Specifications. <https://support.apple.com/en-us/118551>. Accessed: 2024-06-12.
- [22] Ryan Marcus, Andreas Kipf, Alexander van Renen, Mihail Stoian, Sanchit Misra, Alfons Kemper, Thomas Neumann, and Tim Kraska. 2020. Benchmarking Learned Indexes. *Proc. VLDB Endow.* 14, 1 (2020), 1–13.
- [23] Ryan Marcus, Parimarjan Negi, Hongzi Mao, Nesime Tatbul, Mohammad Alizadeh, and Tim Kraska. 2021. Bao: Making Learned Query Optimization Practical. In *SIGMOD Conference*. ACM, 1275–1288.
- [24] Ryan Marcus, Emily Zhang, and Tim Kraska. 2020. CDFShop: Exploring and Optimizing Learned Index Structures. In *SIGMOD Conference*. ACM, 2789–2792.
- [25] openstreetmap [n.d.]. OpenStreetMap. <https://www.openstreetmap.org/>. Accessed: 2024-06-12.
- [26] Joseph O'Rourke. 1981. An On-Line Algorithm for Fitting Straight Lines Between Data Ranges. *Commun. ACM* 24, 9 (1981), 574–578.
- [27] Yehoshua Perl, Alon Itai, and Haim Avni. 1978. Interpolation Search - A Log Log N Search. *Commun. ACM* 21, 7 (1978), 550–553.
- [28] pgm++ [n.d.]. PGM++. https://github.com/qyliu-hkust/bench_search. Accessed: 2024-06-12.
- [29] pgm [n.d.]. PGM-Index. <https://github.com/gvinciguerra/PGM-index>. Accessed: 2024-06-12.
- [30] postgresql [n.d.]. PostgreSQL. <https://www.postgresql.org/docs/current/indexes.html>. Accessed: 2024-06-12.
- [31] pytorch [n.d.]. PyTorch. <https://pytorch.org/>. Accessed: 2024-06-12.
- [32] rmi [n.d.]. rmi. <https://github.com/learnedsystems/RMI/>. Accessed: 2024-06-12.
- [33] Peter Van Sandt, Yannis Chronis, and Jignesh M. Patel. 2019. Efficiently Searching In-Memory Sorted Arrays: Revenge of the Interpolation Search?. In *SIGMOD Conference*. ACM, 36–53.
- [34] Lars-Christian Schulz, David Broneske, and Gunter Saake. 2018. An Eight-Dimensional Systematic Evaluation of Optimized Search Algorithms on Modern Processors. *Proc. VLDB Endow.* 11, 11 (2018), 1550–1562.
- [35] sparksql [n.d.]. Spark SQL. <https://spark.apache.org/sql/>. Accessed: 2024-06-12.
- [36] Chuzhe Tang, Youyun Wang, Zhiyuan Dong, Gansen Hu, Zhaoguo Wang, Minjie Wang, and Haibo Chen. 2020. XIndex: a scalable learned index for multicore data storage. In *PPoPP*. ACM, 308–320.
- [37] tensorflow [n.d.]. TensorFlow. <https://www.tensorflow.org/>. Accessed: 2024-06-12.
- [38] Saravanan Thirumuruganathan, Shohedul Hasan, Nick Koudas, and Gautam Das. 2020. Approximate Query Processing for Data Exploration using Deep Generative Models. In *ICDE*. IEEE, 1309–1320.
- [39] Xiaoying Wang, Changbo Qu, Weiyuan Wu, Jiannan Wang, and Qingqing Zhou. 2021. Are We Ready For Learned Cardinality Estimation? *Proc. VLDB Endow.* 14, 9 (2021), 1640–1654.
- [40] Zhaoguo Wang, Haibo Chen, Youyun Wang, Chuzhe Tang, and Huan Wang. 2022. The Concurrent Learned Indexes for Multicore Data Storage. *ACM Trans. Storage* 18, 1 (2022), 8:1–8:35.
- [41] Nathaniel Weir, Prasetya Ajie Utama, Alex Galakatos, Andrew Crotty, Amir Ilkhechi, Shekar Ramaswamy, Rohin Bhushan, Nadja Geisler, Benjamin Härtasch, Steffen Eger, Ugur Çetintemel, and Carsten Binnig. 2020. DBPal: A Fully Pluggable NL2SQL Training Pipeline. In *SIGMOD Conference*. ACM, 2347–2361.
- [42] wikidata [n.d.]. Wikidata. https://www.wikidata.org/wiki/Wikidata:Main_Page. Accessed: 2024-06-12.
- [43] Samuel Williams, Andrew Waterman, and David A. Patterson. 2009. Roofline: an insightful visual performance model for multicore architectures. *Commun. ACM* 52, 4 (2009), 65–76.
- [44] Chaichon Wongkham, Baotong Lu, Chris Liu, Zhicong Zhong, Eric Lo, and Tianzheng Wang. 2022. Are Updatable Learned Indexes Ready? *Proc. VLDB Endow.* 15, 11 (2022), 3004–3017.
- [45] Jiacheng Wu, Yong Zhang, Shimin Chen, Yu Chen, Jin Wang, and Chunxiao Xing. 2021. Updatable Learned Index with Precise Positions. *Proc. VLDB Endow.* 14, 8 (2021), 1276–1288.
- [46] Shangyu Wu, Yufei Cui, Jinghuan Yu, Xuan Sun, Tei-Wei Kuo, and Chun Jason Xue. 2022. NFL: Robust Learned Index via Distribution Transformation. *Proc. VLDB Endow.* 15, 10 (2022), 2188–2200.
- [47] Xingbo Wu, Fan Ni, and Song Jiang. 2019. Wormhole: A Fast Ordered Index for In-memory Data Management. In *EuroSys*. ACM, 18:1–18:16.
- [48] Xiang Yu, Chengliang Chai, Guoliang Li, and Jiabin Liu. 2022. Cost-based or Learning-based? A Hybrid Query Optimizer for Query Plan Selection. *Proc. VLDB Endow.* 15, 13 (2022), 3924–3936.
- [49] Sepanta Zeighami and Cyrus Shahabi. 2023. On Distribution Dependent Sub-Logarithmic Query Time of Learned Indexing. In *ICML (Proceedings of Machine Learning Research)*, Vol. 202. PMLR, 40669–40680.
- [50] Jiaoyi Zhang and Yihan Gao. 2022. CARMI: A Cache-Aware Learned Index with a Cost-based Construction Algorithm. *Proc. VLDB Endow.* 15, 11 (2022), 2679–2691.
- [51] Ji Zhang, Yu Liu, Ke Zhou, Guoliang Li, Zhili Xiao, Bin Cheng, Jiashu Xing, Yangtao Wang, Tianheng Cheng, Li Liu, Minwei Ran, and Zekang Li. 2019. An End-to-End Automatic Cloud Database Tuning System Using Deep Reinforcement Learning. In *SIGMOD Conference*. ACM, 415–432.
- [52] Jiaoyi Zhang, Kai Su, and Huanchen Zhang. 2024. Making In-Memory Learned Indexes Efficient on Disk. *Proceedings of the ACM on Management of Data* 2, 3 (2024), 1–26.
- [53] Zhou Zhang, Zhaole Chu, Peiquan Jin, Yongping Luo, Xike Xie, Shouhong Wan, Yun Luo, Xufei Wu, Peng Zou, Chunyang Zheng, Guoan Wu, and Andy Rudoff. 2022. PLIN: A Persistent Learned Index for Non-Volatile Memory with High Performance and Instant Recovery. *Proc. VLDB Endow.* 16, 2 (2022), 243–255.
- [54] Rong Zhu, Wei Chen, Bolin Ding, Xingguang Chen, Andreas Pfadler, Ziniu Wu, and Jingren Zhou. 2023. Lero: A Learning-to-Rank Query Optimizer. *Proc. VLDB Endow.* 16, 6 (2023), 1466–1479.